Barcoded Magnetic Tiles for Programmable Assemblies*

Urmi Majumder† and John H. Reif‡

Abstract: As manufacturing scales down, there is an increasing need to use bottom-up self-assembly techniques over conventional top-down assembly techniques. Previously self-assembling units or tiles forming aggregates based on the polarity of magnetic pads on their sides have been demonstrated. These assemblies were simple, primarily because of the small variety of magnetic pads used. This paper addresses the key challenge of increasing the variety of magnetic pads for tiles, which would allow macroscopic tiles to self-assemble into more complex patterns. The main contribution of our paper is a novel barcode scheme for magnetic tile pads, and the design and optimization of our barcode scheme for magnetic pads is the paper's major concern and focus. We present a physical model and a software simulation system that models the binding of these tiles using magnetic interactions as well as external forces. The physical model is based on Newtonian mechanics and Maxwellian magnetics. The simulation system models attachment, orientation and binding of macroscopic tiles using magnetic interaction as well as external forces (wind) which provide energy to the system. It allows us to estimate the suitable parameters for the barcode scheme for magnetic pads that selectively bind (or do not bind) with other tiles, and so to calculate the predicted interactions for two large floating

*This paper is a revised version of the conference proceedings paper: Urmi Majumder and John H. Reif, A Framework for Designing Novel Magnetic Tiles Capable of Complex Self-Assemblies, Conference on Unconventional Computation, Vienna, Austria, Aug 25-26, 2008, Unconventional Computing, Lecture Notes in Computer Science number 105633, Springer, Berlin Heidelberg.

†Oracle Corporation, Washington D.C, USA

‡Department of Computer Science, Duke University, Durham, NC , USA and Adjunct, Faculty of Computing and Information Technology (FCIT), King Abdulaziz University (KAU), Jeddah, Saudi Arabia

tiles with embedded magnets. We observed that tiles that are elongated and magnetically shielded allow less cross-talk between interactions and the implementation of a magnetic bar-code for a larger number of specific bindings. We also demonstrate how we can use our simulation model to extract a scalable thermodynamic model which can be used to predict yield of assembly on a larger scale and also to provide better insight into the dynamics of our physical system.

1 Introduction

Self-assembly is a process where small components spontaneously organize themselves into a larger structure. This phenomenon is prevalent on all scales, from molecules to galaxies. Though self-assembly is a bottom-up process not utilizing an overall central control, it is theoretically capable of constructing arbitrarily complex objects.

One of the most well-studied sub-fields of self-assembly is molecular self-assembly. However, many interesting applications of self-assembling processes can be found at a larger scale, such as micro - mm scale. Massively parallel self-assembling systems present a promising alternative to conventional pick-and-place manufacturing. There are many examples of self-assembling systems at this scale which may be relevant to robotics and manufacturing such as self-assembled monolayers, the patterned assembly of electronic components and MEMS devices and the assembly of micro-robots or sensors.

This paper explores magnetic self-assembly with the ultimate goal of discovering the practical applications towards manufacturing and computing systems. Most of the related work described in Section 2.2 focuses on the demonstration of macro- and micro-scale self-assembly. However, this paper focuses more on the *design* issues relevant to the generation of more complex structures using our novel *barcode scheme*. In particular, this paper address the key challenge of increasing the variety of magnetic pads for tiles, which will allow the tiles to self-assemble into patterns of increased complexity governed by the selection of the pads of the tiles. In fact, the introduction of our barcode scheme

potentially allows for the generation of arbitrary complex structures using magnetic self-assembly at the macro-scale.

2 Overview of Macro-scale Massembly

2.1 Why use Macro-scale Self-Assembly

Goerge Whitesides, one of the principal figures in the field of self-assembly, proposed a number of reasons to consider the self-assembly of macroscopic components [**?**]. He suggested that macroscopic self-assembly would allow the study of the assembly process in a way that cannot be performed on the molecular scale, which would, in turn, help us understand the principles of self-assembly. Additionally, the flexibility and range of interactions is much greater at larger scales.

As we will see in Section 2.2, self-assembly in the macro and meso (sub millimeter range) scale has been demonstrated using a variety of interactions such as capillary interaction [**? ? ?**], magnetic interaction [**? ? ?**], electrostatic interaction [**? ? ?**] and many others. Furthermore, it is often easier to fabricate and characterize devices at the micro and macro scale rather than at the nano-scale. However, the more lucrative reasons for using self-assembly as a synthesis technique in the macro-scale may be that 1) macro-scale self-assembly allows fabrication of 3D objects [**? ? ?**] while photolithography, the process by which computer chips are manufactured today is intrinsically a planar technology and 2) self-assembly may be of great aid to conventional robotic pick-and-place assembly by offering the opportunity to form structures in regions inaccessible to robotic arms. Hence, in this paper we describe how we can apply our collective knowledge of building DNA-based self-assembled nanostructures to another scale and using a binding mechanism other than hybridization, namely magnetic force and develop a framework for building complex macro-scale magnetic assemblies.

2.2 Previous Work in Macro-scale Self-Assembly

Recent work in the field of macro-scale self-assembly include development of systems based on capillary interactions among millimeter-scale components either floating at a fluid-fluid interface or suspended in an approximately iso-dense fluid medium [**?** **?** **?** **?** **?** **?** **?** **?** **?**]. Rothemund [**?**] demonstrated the use of hydrophobic and hydrophilic interactions to generate self-assemblies of moderate complexity and scale. His work was notable since it is the only work which demonstrated computational self-assembly at the macro-scale.

2.2.1 Magnetic Passive and Active Assemblies

Magnetic assembly [**?** **?** **?**] is a form of macro-scale self-assembly that is directed by magnetic dipole interaction. One successful application of magnetic assembly is the spontaneous folding of elastomeric sheets, patterned with magnetic dipoles, into free standing, 3D spherical shells [**?**]. This technique has been shown to generate relatively simple structures, largely due to the limited nature of the magnetic interactions. This kind of self-assembly is also known as *passive self-assembly* since assembly takes place without external control. Here we address the key challenge of going beyond such limitations and aim to design more complex structures via magnetic assembly. To increase the complexity of magnetic assemblies, Klavins *et al.* [**?**] developed programmable units that move passively on an air-table and bind to each other upon random collisions. These programmable units have on-board processors that can change the magnetic properties of the units dynamically during assembly. Once attached, they execute local rules that determine how their internal states change and whether they should remain bound based on the theory of graph grammars [**?**]. This form of assembly is referred to as *active assembly*. However, our goal is to generate complex magnetic assemblies without the use of on-board processors which we refer to as *passive assembly*. This form of magnetic assembly is very similar to standard techniques for molecular assembly, which are driven by pre-programmed bonds (e.g. Watson-Crick complementarity) and are mixed by thermal forces.

3 Our Contribution

The goal of this paper is to develop techniques that will allow the self-assembly of complex structures at the macro-scale. This task is quite challenging, since the available binding mechanisms (using magnetic and capillary interaction) currently used at the macro-scale provide only for binary binding (e.g., positive and negative in the case of magnetic binding and hydrophobic/hydrophilic interactions in the case of capillary binding). By contrast, DNA provides a large number of specific bindings through the use of complementary pairs of DNA sequences that can hybridize selectively. Here, we mimic the techniques and principles of molecular self-assembly to build complex structures at the macroscopic level. See Section A in the appendix on related work in molecular self-assembly. The key challenge then is to extend the binding mechanisms at this scale to a much larger number of specific bindings, rather than just two. We achieve this by using a *magnetic barcode* technique described in this paper. In general, in this paper we explore magnetic self assembly with the ultimate goal of dis- covering the practical limits for its use in the manufacturing and computing systems. Most of the related work described above is focused on the demonstration of macroscale self-assembly. However, as we mentioned earlier, here we emphasize more on the design issues relevant to the generation of more complex structures using our novel barcode scheme.

Our testbed is an example of a distributed system where a large number of *relatively simple components* interact locally to produce interesting global behavior. Square *programmable tiles* float passively on a forced air-table, mixed randomly by oscillating fans which simulate Brownian motion of a macroscopic scale. The tiles have a magnetic encoding on each of their faces. When they collide, if the facing poles are exactly complementary, the tile faces bind to each other and this process repeats to generate our desired final structure. If the tiles collide but do not match exactly, the tiles will tend to repel each other. The actual resulting motion is quite complicated and will be discussed further in Section 5.1.1.

We discuss how our barcode scheme relates to achievable shapes and how we can optimize our tile design. We further describe how the testbed system can be modeled

using a *rigid-body simulation*. We have used this simulation environment to perform a preliminary validation of the feasibility of using magnetic tiles (with barcoded pads) to generate patterned lattices. We conclude with a discussion on scalability issues and how we can use our simulation results to predict yields in larger scales.

3.1 Organization of the Paper

We have organized our contribution in the following manner: section 4 describes the magnetic self-assembling system. Specifically, Section 4.1 describes the overall scheme while Section 4.2 discusses the barcode scheme and the set of achievable shapes. Section 4.3 next discusses the various combinatorial, thermodynamic and physical optimization rules that can be applied to improve the yield of assembly. Additionally, Section 4.4 presents techniques from robot motion planning that can improve tile designs. Section 5 presents the simulation model (Section 5.1.1) and some preliminary results (Section 5.2) from simulating a simple two-tile system. It also discusses the feasibility of extracting a higher level kinetic model (Section 5.3.1) based on assembly/disassembly rates from the low level physical simulation model and includes a discussion on scaling of the system (Section 5.3.2), yield optimization (Section 5.3.3) and errors in assemblies (Section 5.3.4). Finally, Section 6 concludes the paper.

4 Design of a Magnetic Self-Assembly System

Self-assembly at the macro-scale can happen through a wide range of binding forces viz. gravitational, electrostatic, magnetic, capillary, etc, that provide bind together components in the assemblies. Past research has focused on using capillary interaction as a binding force [**?**]. Now the choice of the binding force depends on several factors like scale and magnitude of the force, environmental compatibility and influence of the interactions on the function of the system. We have chosen to use magnetic force as the binding force for our self-assembling system mainly because magnetic interactions are insensitive to the surrounding medium and are independent of surface chemistry. Also, careful engineering of magnetic forces can control the long and short range interactions between components.

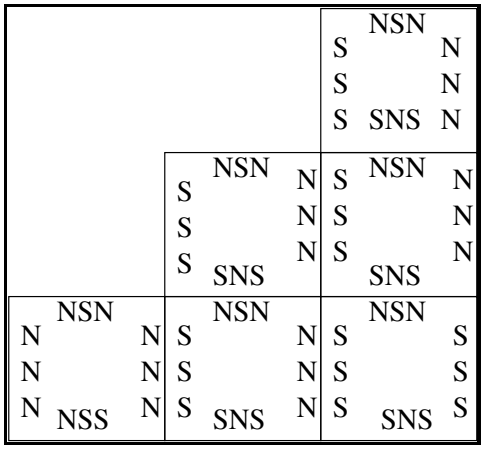

Figure 1: **A typical magnetic assembly**

This is important because a key issue in the design of programmable self-assembly is the recognition between components, governed by the design, surface chemistry and topology of the interacting surfaces.

4.1 The Overall Scheme

The overall design of our system is as follows: the main component of our self-assembling system is a set of square tiles. Each edge of a tile is lined with a sequence of magnetic dipoles, aligned perpendicular to the tile edge and can face either the north or south pole out. A typical encoding on a tile face may be {NNNS} where N or S denotes whether the north pole or the south pole of the dipole is facing out of the tile. The tiles float on a custom-made air-table, equipped with a set of fans to mix the tiles. Thus all the interactions between the tiles are due to chance collisions. The idea is that if a tile face (e.g. with encoding {NNNS}) collides with a tile face with matching encoding (i.e. {SSSN}), they stick together, thus resulting in an assembly [Figure 1].

4.2 The Barcode Scheme and Achievable Shapes

In the context of our magnetic self-assembly a *barcode* is a series of bar magnet poles that face out of the tile on any face (e.g. NSN and SNS as in Figure 1). If we have a n character long barcode on each face of every square tile in our tile set then number of distinct tiles is 2^{4n}. However, there can be different types of assemblies ranging from *uniquely addressable* to *homogeneous*. A uniquely addressable lattice is where each tile in the assembly has a unique location. Any such lattice of size $m \times n$ calls for $m(n-1) + n(m-1)$ different barcodes. Thus, in this case, we need barcode of length $O(log(mn))$. At the other extreme lie homogeneous lattices which call for exactly one tile type and can be constructed with $O(1)$ length barcodes. In between these two extremes lie computational assemblies, which have been shown to be Turing Universal [**?**]. Here we treat each tile as a computational unit where the east and south faces are inputs of the computation while north and west are outputs of the computations, which are then used in the next step of the computation. In other words, in Winfree's Tile Assembly Model (TAM), a tiling assembly of size nT simulates a given Blocked Cellular Automaton of size n running in time T [**?**]. For any such computation, a barcode of length n generates a tile set of size 2^{2n}. Further the number of functions we can have is $(2)^{2^{2n}}$.

Some examples of complex assemblies are shown in Figure 2. Each of these assemblies are based on Winfree's Tile Assembly model [**?**] and only uses a small number of tile types ($O(1)$), as is the characteristic of any computational assembly.

The barcode scheme automatically leads to the question of complexity of achievable shapes. The problem of size complexity of a self-assembled shape was first addressed by Rothemund and Winfree [**?**] for computational molecular assembly. However, their results also hold for macroscopic assemblies. Suppose that τ is defined as the parameter which decides when to add a tile to a growing assembly. In particular, when the total interaction strength of a tile with its neighbors exceed τ, the tile is added to the assembly. Then the minimum number of distinct tiles required to self-assemble a $N \times N$ square decreases from N^2 to $O(logN)$ tiles as τ is increased from 1 (noncooperative bonding) to 2 (cooperative bonding). An alternative measure is to compute the minimum number of

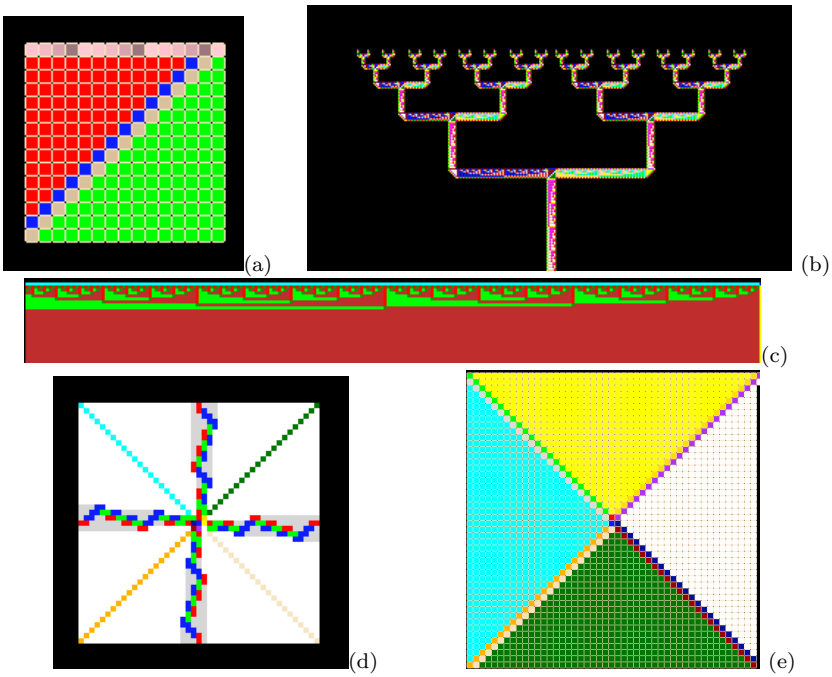

Figure 2: **Examples of Complex Assemblies: (a) Unary Square, (b) Binary Tree, (c) Binary Counter, (d) Beaver Square, (e) Spiral, made with XGROW [?].**

distinct side labels used for assembling the square. It is still an open question whether both measures give asymptotically similar results. The latter will be more useful for a practical implementation of the system since, in reality, the number of distinct binding interactions is limited due to imperfect specificity of binding. It should be mentioned here that Adelman *et al.* [**?**] later proved a tighter bound of $\Theta(\frac{logN}{loglogN})$ for the minimum number of distinct tiles required to assemble a $N \times N$ square uniquely, by demonstrating that self-assembly can compute changes in the base representation of numbers. A further decrease was achieved by Kao *et al.* [**?**] who proved that using a sequence of $O(m)$ changes in τ (where m is an arbitrarily long binary number), a general tile set of size $O(1)$ can uniquely assemble any $N \times N$ square.

For arbitrary shapes (e.g. non-squares) no such tight bounds exist as yet. However, Soloveichik *et al.* [**?**] recently showed that the minimal number of distinct tile types required to self-assemble an arbitrarily scaled structure can be bounded both above and below by the shape's Kolmogorov Complexity where Kolmogorov Complexity of a string

I is defined to be the length of the shortest program that computes or outputs I, when the program is run on some fixed reference Universal computer.

4.3 Tile Programming

This section describes our barcode design scheme. We will sometimes refer to the barcode on a tile face as a *word*. Here our goal is to design a set of words such that the energy difference between a pair of perfectly matched faces and a pair of partially or completely unmatched faces is maximized. Tulpan *et al.* [**?**] proposed a DNA-design algorithm based on local search approach that can be utilized for our magnetic barcode design with minimal modifications. The algorithm takes as input: the length of each code word, the number of unique codewords that need to be generated and a set of constraints that the output set must satisfy. We describe some of the constraints for magnetic tile design below.

4.3.1 Combinatorial Optimization

Some examples of combinatorial constraints [**?**] are: (1) the number of mismatches in a perfect alignment of two tile faces must be above an user-defined threshold. For instance if a tile face encoded as NNNN aligns up with a face encoded as SNSN then there will be two mismatches in such an alignment. Note that mismatches need not be consecutive and can be minimized using prefix codes and Hamming distance maximization. (2) The number of mismatches between a perfect alignment of one tile face encoding and the complement of another tile face encoding should also be above some threshold. (3) The situation of tile binding can be made more complicated by the presence of a slide match configuration (e.g. when a tile face bearing NNNSSNSNSN matches with another tile face bearing NNSNSNSNNS starting at the fourth location on the second face and the first one for the first tile). Hence the number of mismatches in a slide of one tile face over another must be above some threshold. The problem of slide match configuration can be handled using shift distinct codes or complementary shapes for tile faces. (4) The maximum number of consecutive matches between all slides of one tile face encoding over the other must be in an user defined range.

4.3.2 Thermodynamic Optimization

Thermodynamic constraints are based on the free energy of a pair of tiles binding. The free energy of an assembly is not just a function of the encodings, but also the number, orientation and speed of fans and number of tiles. However, any model incorporating so many free parameters will be quite complicated. Hence, for simplicity, we will assume that the sole contributor to free energy in our case is the magnetic interaction between two tile faces when they are perfectly aligned. Effects of adjacent faces (e.g. north and east) can be neglected because of shielding (Section 5.1.2). Some thermodynamic constraints used in the algorithm [**?**] are: (1) the free energy of a perfect match must be below a given threshold. (2) The free energy of a code word and the complement of another code word, two words or two complements must also be in a desired range.

Eventually, the goal is to obtain a positive free energy gap between the perfect match and imperfect matches of a code word. Since our magnetic assembly is a mechanical system, we will also take some physical factors into consideration while designing tiles.

4.3.3 Physical Optimization

We can minimize intra and inter-magnetic cross-talk using the following techniques [Figure 3]: (1) Large tile to magnetic dipole size ratio (minimizes interaction between adjacent tile faces). (2) Barcodes towards the center of the face (minimizes interaction between adjacent tile faces). (3) Use of spacer sequences, that seperate the magnets used for binding tiles. (4) Use of magnets, enlongated allong their magnetic axis, essentially minimizing the effect of one pole on another. (5) Use of magnetic shields. (a coating of soft iron on the magnets prevents coupling of flux lines between two adjacent bar magnets). An alternative method is to use *Halbach array*, which is a special arrangement of permanent magnets that augments the magnetic field on one side of the device while canceling the field to near zero on the other side [**?**]. Although in this scheme we can intensify the magnetic field at the end of the tile faces and minimize it at the other end of magnetic arrangement, the method cannot handle sideways magnetic crosstalk.

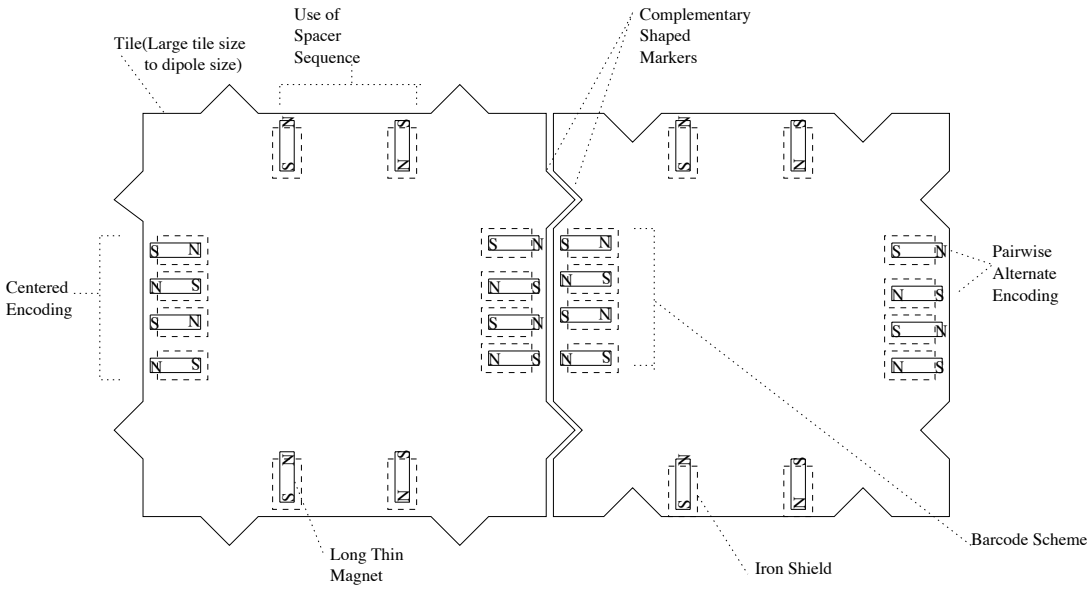

Figure 3: **Techniques for minimizing magnetic crosstalk.**

4.4 Improving Tile Designs using Motion Planning Studies

Complementary shape matching [Figure 3] is a useful technique in optimal tile design [**?**]. We can verify the "goodness" of a match using a motion planning technique called a *probabilistic roadmap* [**?**] which is mostly used to check the connectivity of a collision free path in a high-dimensional space. It can also be used to capture the extrema of a continuous function (e.g. potential energy) over high-dimensional space [**?**] since this map captures the connectivity of the low energy subset of the configuration space in the form of a network of weighted pathways. In our context, it can be used to study the potential energy landscape of a two tile assembly. Specifically it will be interesting to find out whether an energetically favorable path exists between any randomly generated configuration for the tiles and its final bound state and if it exists, compute the energy barrier. Further, it may be useful to study how the energy barrier varies with various complementary shapes and depth of the binding site.

The conformational space for a two-tile system with one fixed tile and another with some initial velocity is essentially three-dimensional (x, y and θ). The energy function is

based on the magnetic interaction model (See Sect. 5.1.1). Milestones in this configuration space are generated randomly using rejection sampling where the probability of accepting a milestone depends on the tile configuration. An edge exists between any two milestones in the configuration space if the path between them is energetically favorable and the weight is determined by the energy of the path. Once the graph is constructed there are many ways to use it. One typical query is the shortest weight path between two configurations; another query is to use the graph to characterize a true binding site based on the energy barrier mentioned above.

It should be mentioned here that several other geometric methods have been developed to study the general shape matching problem that can be applied to optimal tile design as well. Two such methods are the *surface matching* technique [**?**] and the *object recognition* technique [**?**]. In the first technique, two tiles would be matched if there is a correspondence between the points on their surface, meaning that rigid body transformations applied to one tile can achieve point to point contact between the two tile surfaces. Then the goal is to find the maximum match between two such tile surfaces. In the second technique, given one or more object models and a scene containing images of the objects, the problem is to determine if the same object appears in the scene and if so where it occurs. In the context of tile binding, the moving tile may be thought of as the object model. Then a collection of points on the fixed tile corresponds to the images. The goal is to compute a rigid body transformation that would align as much of the image data as possible with one of the supplied object models.

5 Simulation of a two tile system

5.1 Simulation Model

5.1.1 The Physical Model

Since actual experimentation would require elaborate patterning of tiles and careful placement of fans with appropriate binding force, we evaluated our barcode scheme by simulating a two-tile assembly. This section presents the physical model underlying the

simulation. The central component of our tile motion model is an air-table. that provides a two-dimensional fluid environment for the tiles. As tiles traverse the testbed, they will lose kinetic energy due to friction and variations in their air cushion. In our model, we assume that our air-table surface has a very low coefficient of friction, minimizing energy losses as the tiles traverse on the air-bed.

Fans around the air table are used to agitate the tiles, providing kinetic energy to drive the assembly. To model the fans, our simulation makes the simplified assumption that the the potential energy E_f is a negative exponentially decaying function of the distance $\overrightarrow{r}$ from a tile to a fan, and takes the form $E_f = e^{-|r|^2}$. This simplified assumption may be justified by an assumption of negative exponentially decaying dispersion of the fan's energy around it. Hence, the fan force can be obtained as the gradient of potential energy. Interestingly, the oscillating fans simulate the Brownian motion which provides the kinetic energy behind diffusion and self-assembly in the molecular level.

For modeling tile collision we assume that the coefficient of restitution between two tiles is small enough to let short-range magnetic forces determine whether a binding event will take place or not. Our friction model is essentially an approximation of Coulomb's friction model. In particular, care should be given such that *compliant motion* is guaranteed. A basic principle of Newtonian mechanics states that when the tile exerts force directly on to the surface of the air-table, the latter exerts a reaction force on the tile as well. Now if the applied force points into the surface of the air-table, the reaction force will cancel the former. For any other direction of the applied force, the tile may slide on the air-table. The force applied by the tile can be parallel to the surface as well. In general, the applied force can be decomposed into parallel and perpendicular components. If the parallel component is too small compared to the perpendicular component, the tile will get stuck on the surface. Compliant motion is when motion occurs smoothly and, hence, care should be given such that tiles do not stick to the air-table surface. Note that this principle applies to inter-tile friction as well.

5.1.2 Magnetic Interaction Model

The magnetic strips glued to the sides of the tiles drive the tile movements in the airbed apart from the fans around the air-table. Hence, modeling these magnetic interactions correctly is key to predict the extent of binding. Since the magnets are glued to the tile surface and are shielded, intra-tile magnetic interaction is negligible. For interfacing tiles, our design ensures that only the magnets on the nearest face will have any effect on a given bar magnet.

Magnetic Dipole Approximation : We approximate our bar magnets as magnetic dipoles. We do not have any source of electric current in our system; so Maxwell's equations for magnetostatics apply in this case specifically, $\overrightarrow{\bigtriangledown} \cdot \overrightarrow{B} = 0$ and $\overrightarrow{\bigtriangledown} \times \overrightarrow{B} = \frac{4\pi}{c}\overrightarrow{J}$ where $\overrightarrow{B}$ is the flux density of the magnet and $\overrightarrow{J}$ is its electric current density. If we define $\overrightarrow{B} = \overrightarrow{\bigtriangledown} \times \overrightarrow{A}$, then for single geometries we can perform Coulomb-like integrals for $\overrightarrow{A}$ and then a multi-pole expansion of it up to the dipole term, yielding flux density $\overrightarrow{B} = \frac{3(\overrightarrow{m}.\hat{r})\hat{r} - \overrightarrow{m}}{\overrightarrow{r}^3}$ at a distance $\overrightarrow{r}$ due to a magnet with dipole moment $\overrightarrow{m}$. Hence the force on a dipole in an external magnetic field is $\overrightarrow{F} = \bigtriangledown(\overrightarrow{m}.\overrightarrow{B})$. In particular, suppose we want to compute the force experienced by a magnet M_1 on tile T_1 due to the magnetic field $\overrightarrow{B}_2$ of a magnet M_2 on tile T_2 located at a distance $\overrightarrow{r} = xi + yj$. Let the dipole moment of a magnet M_1 be $\overrightarrow{m}_1 = m_{x1}i + m_{y1}j$ and that of M_2 be $\overrightarrow{m}_2 = m_{x2}i + m_{y2}j$. Then,

$$\begin{aligned} \overrightarrow{B}_2 &= \frac{3(\overrightarrow{m}_2.\hat{r})\hat{r} - \overrightarrow{m}_2}{\overrightarrow{r}^3} \\ &= \frac{3(m_{x2}x^2 + m_{y2}xy)i + 3(m_{x2}xy + m_{y2}y^2)j}{(x^2+y^2)^{\frac{5}{2}}} - \frac{m_{x2}i + m_{y2}j}{(x^2+y^2)^{\frac{3}{2}}} \end{aligned} \quad (5.1.1)$$

Consequently,

$$
\begin{aligned}
\overrightarrow{F} &= \bigtriangledown(\overrightarrow{m}_1.\overrightarrow{B}_2) \\
&= \bigtriangledown\Big(3\frac{(m_{x1}m_{x2}x^2 + m_{x1}m_{y2}xy) + (m_{y1}m_{x2}xy + m_{y1}m_{y2}y^2)}{(x^2+y^2)^{\frac{5}{2}}} \\
&\quad -\frac{(m_{x1}m_{x2} + m_{y1}m_{y2})}{(x^2+y^2)^{\frac{3}{2}}}\Big) \\
&= \Bigg(-15x\frac{(m_{x1}m_{x2}x^2 + m_{x1}m_{y2}xy) + (m_{y1}m_{x2}xy + m_{y1}m_{y2}y^2)}{(x^2+y^2)^{\frac{7}{2}}} \\
&\quad +\frac{3(2m_{x1}m_{x2}x + m_{x1}m_{y2}y) + 3m_{y1}m_{x2}y}{(x^2+y^2)^{\frac{5}{2}}} + \frac{3x(m_{x1}m_{x2} + m_{y1}m_{y2})}{(x^2+y^2)^{\frac{5}{2}}}\Bigg)i \\
&\quad +\Bigg(-15y\frac{(m_{x1}m_{x2}x^2 + m_{x1}m_{y2}xy) + (m_{y1}m_{x2}xy + m_{y1}m_{y2}y^2)}{(x^2+y^2)^{\frac{7}{2}}} \\
&\quad +\frac{3m_{x1}m_{y2}x + 3m_{y1}m_{x2}x + 6m_{y1}m_{y2}y}{(x^2+y^2)^{\frac{5}{2}}} \\
&\quad +\frac{3y(m_{x1}m_{x2} + m_{y1}m_{y2})}{(x^2+y^2)^{\frac{5}{2}}}\Bigg)j \qquad (5.1.2)
\end{aligned}
$$

We can compute the dipole moment of a bar magnet of length l and square cross-sectional area with $a = 4r^2$ as follows. With long thin magnets, we can approximate the bar magnet with a cylindrical bar magnet which can be further approximated by a solenoid which is l units long, has N turns each of which has area πr^2 sq units and current i. The magnetic field at the end of the coil is $B_0 = \frac{\mu_0 N i}{2\sqrt{l^2+r^2}}$ and following the analogous calculation for an electric dipole, the magnetic dipole moment $|M| = \frac{2B_0 al}{\sqrt{l^2+r^2}}$ and the direction is from the north pole to the south pole. In our case the $|M|$ is same for all magnets and can be set to some pre-defined value.

FEMM Simulations : We used *Finite Elements Method Magnetics*[1] to verify the effect of all the techniques described above. FEMM has a much greater capacity to represent physical situation than the rigid body simulation. The results in Figure 4 provides some evidence that magnetic shielding may be an effective technique for minimizing magnetic crosstalk. The near-blue color indicates a magnetic field density in the range of $4.986E-005$ to $1.022E-001$, and the black lines indicate the field flux lines within this range, at increments of magnetic field density $1.000E-004$. The magnetic tile on the left is indicated

[1] http://femm.foster-miller.net/

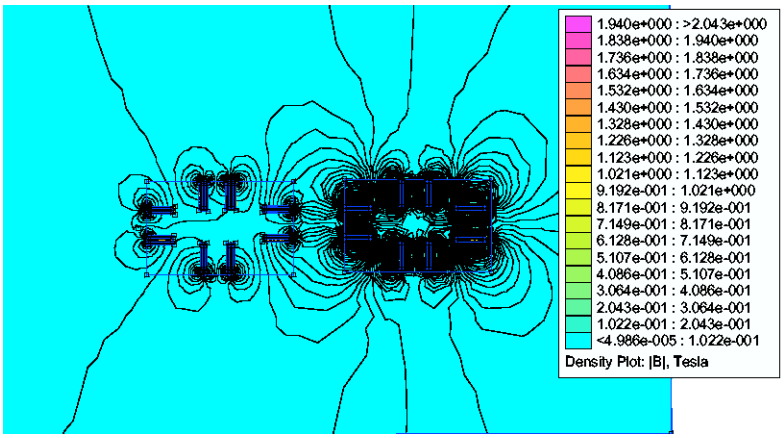

Figure 4: **FFEMM Simulations demonstrating the effect of magnetic shielding of the magnetic tile on the left, and lack of magnetic shielding of the magnetic tile on the right.**

by a lightly outlined rectangle whereas the magnetic tile on the right is indicated by a darkly outlined rectangle. The magnetic tile on the right has no magnetic shielding, and as a result of the lack of magnetic shielding, the magnetic tile on the right has a large number of field lines penetrating it, resulting in low magnetic crosstalk. In contrast, the magnetic tile on the left has been provided magnetic shielding around its sides, with the dipoles exposed, and as a result of this magnetic shielding, the magnetic tile on the left has few field lines penetrating it, resulting in low magnetic crosstalk.

Observe that the field lines are less dense in the left tile with magnetic shielding, which indicates that the attractive forces used for assembly are also weakened as a result of the magnetic shielding. However, this can be compensated by correspondingly more powerful magets.

5.1.3 Tile Motion Model

Once the individual forces have been calculated, we can model the tile motion. On the testbed, a tile's motion is described in terms of its two-dimensional linear acceleration $(\frac{d^2x}{dt^2}, \frac{d^2y}{dt^2})$ and one-dimensional angular acceleration $(\frac{d^2\theta}{dt^2})$:

$$\begin{pmatrix} \frac{d^2x}{dt^2} \\ \frac{d^2y}{dt^2} \\ \frac{d^2\theta}{dt^2} \end{pmatrix} X = \begin{pmatrix} -\mu & 0 & 0 \\ 0 & -\mu & 0 \\ 0 & 0 & -\mu \end{pmatrix} \begin{pmatrix} \frac{dx}{dt} \\ \frac{dy}{dt} \\ \frac{d\theta}{dt} \end{pmatrix} + \frac{\overrightarrow{F_m}(x,y)}{m} + \frac{\overrightarrow{\tau_m}(\overrightarrow{r}, \overrightarrow{F_m})}{I} \tag{5.1.3}$$

where m is the mass of the tile, I is the moment of inertia about the axis passing through its centroid perpendicular to the bed, μ is the coefficient of friction, $\overrightarrow{F_m}$ is the magnetic dipole force, $\overrightarrow{\tau_m}$ is the torque exerted on the tile by the force $\overrightarrow{F_m}$ acting at the magnetic point $\overrightarrow{r}$ relative to the tile's center of mass. For simplicity, we simulate applying the fan force to the center of the tile making the torque of the fan force equal to zero. Tiles also receive impulse forces and torques when they collide with each other or the sides of the air-table. By Newton's equations, the force and torque imparted during these events conserve linear and angular momentum; however the kinetic energy is not conserved, since the collisions are partially inelastic.

5.2 Preliminary Simulation Results

Our simulation uses the Open Dynamics Engine[2] library, which can compute trajectories of all the tiles and determine the results of the collisions. The goal of our simulation is to discover the range of the magnetic force effective for tile binding in the absence of wind energy. Here, the initial position of a first tile is fixed with zero initial velocity. The other second tile has an initial random position and we gave the second tile some initial velocity. We then computed the likelihood of a correct match, given the kinodynamic (position, orientation and velocity) constraints on this tile. Note that by providing the random initial velocity we are essentially simulating the exponentially decaying potential function of the wind energy source. Recall that in our simulation, we call two tile faces connected if the corresponding matching dipoles are within some pre-defined threshold distance. Also, for estimating the likelihood of match in any simulation, we declare the tiles connected only when they remain connected until the end of the simulation.

Our air-bed is 2 m wide and 2 m long. The air-table has a very small coefficient of friction, specifically 0.0005. The dimension of a tile is $43 \times 43 \times 1.3\ cm^3$ while that of each

[2]http://ode.org

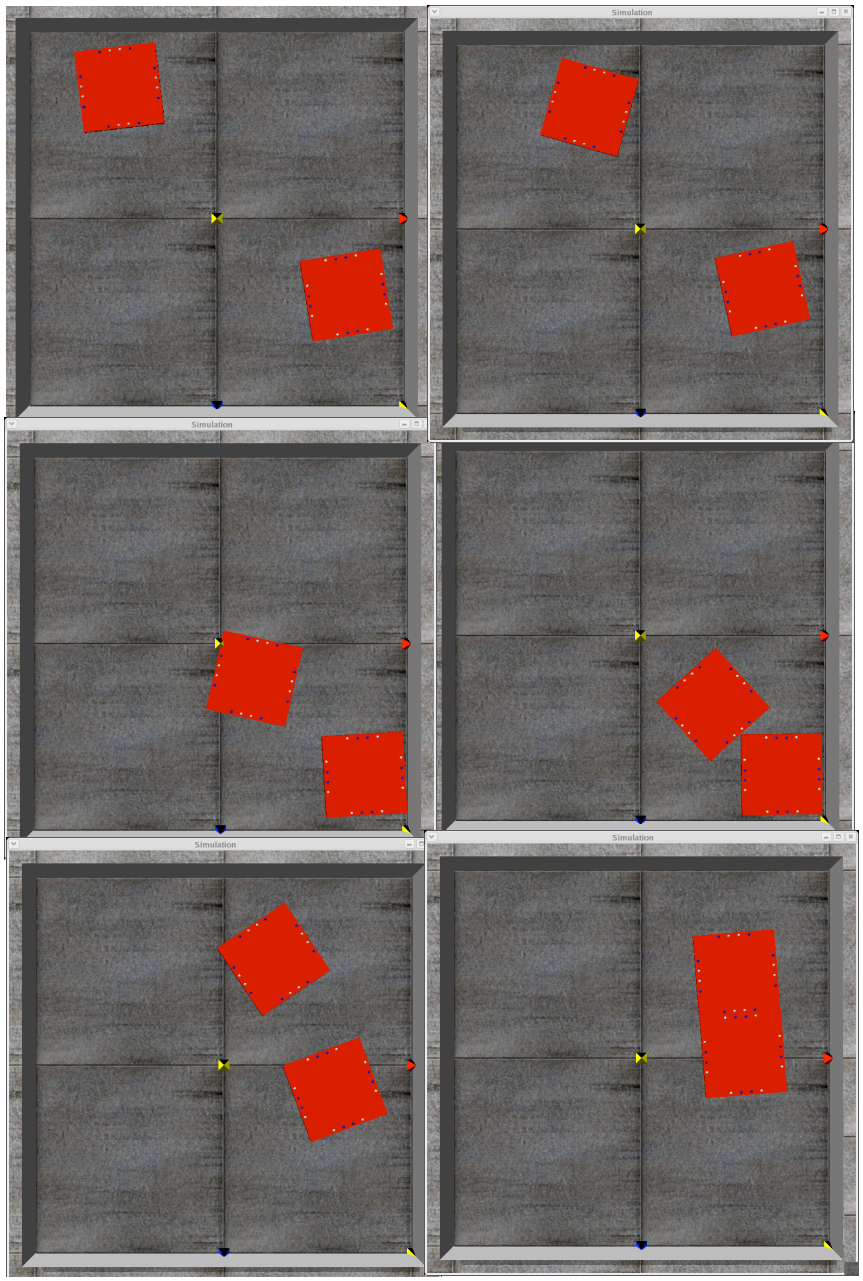

Figure 5: **(Top to Bottom, Left first, then Right) A simulation snapshot of two self-assembling square magnetic tiles (decorated with four bar magnets on each face and without complementary shapes) based on the original simulator from Klavins *et al.* [?].**

bar-magnet is $1 \times 1 \times 0.3\ cm^3$. This ensures a large tile to dipole size ratio. Each tile has a mass of 100 g. The frictional coefficient between two tile surfaces is assumed to be 0.3 while the coefficient of restitution for inter-tile collision is 0.01. An example simulation of a two-tile assembly is shown in Figure 5.

Since the emphasis in this work is the design framework, only preliminary simulation results are presented.

5.3 Interpretation of Simulation Data

5.3.1 Kinetic Model

The low-level simulation model based on Newtonian mechanics and Maxwellian magnetics serves as the basis for a higher level kinetic model based on on/off rates, very similar to chemical kinetics [**?**]. Chemical kinetics is useful for analyzing yields in large assemblies and understanding assembly dynamics without having to consider the innumerable free parameters in the low-level physical model. Although the number of tiles in our preliminary experimental setup is quite small and is not very suitable for deducing higher level model parameters, the goal here is to establish the feasibility of the process. For this purpose, we needed a stochastic model for tile attachment events. Since we can to first order assume the tile attachment events in a given time interval are independant, we modeled tile attachment by a Poisson process where the on-rates λ_{on} are exponentially distributed.

The purpose of the Figure 6 is to simply indicate the likelihood of a pair of tiles moving to correct match configurations for a range of initial relative orientations (where the relative orientation is on the range $(-1, 1)$) and initial relative velocities (where the relative velocity is on the range $(-1, 1)$), and x is on the range $(0, 1)$ and y is on the range $(0, 1)$.To generate this Figure, we used simulation data obtained from the above simulation using the Open Dynamics Engine, and then used Monte Carlo Integration to estimate the on-rates λ_{on}. Similarly, the off-rate can be determined using the data on time interval between when the tiles are attached and disconnected. In particular, Figure 6 illustrates the probability distribution for the event that the assembly simulation of the

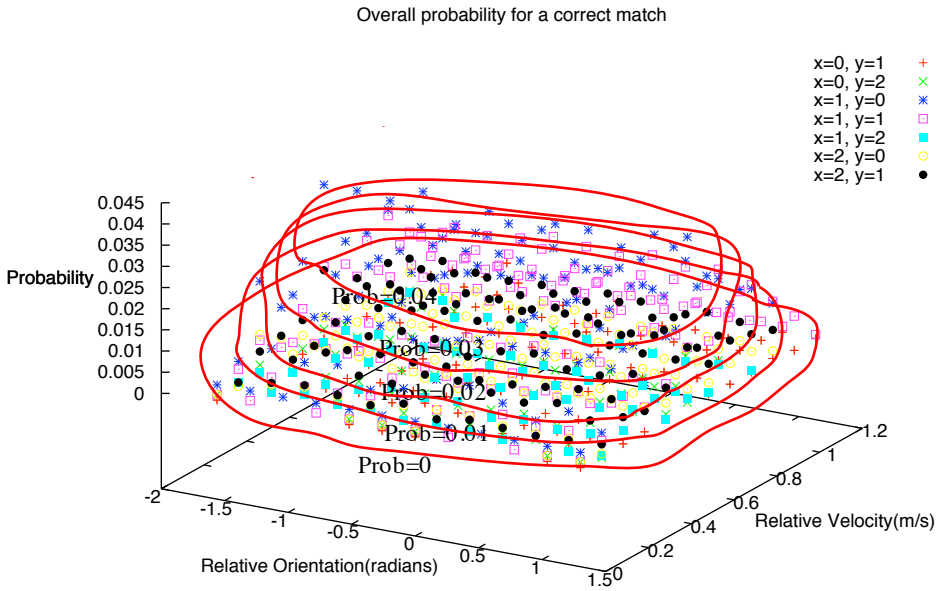

Figure 6: **A 3d dot plot of probability distribution of likelihood of a pair of tiles moving to correct match configurations for a range of initial relative orientations from -1.5 to 1.5 radians and range of relative velocities from 0 to 1.3 m/s. The red countour lines indicate probabilities at intervals of 0.01.**

two tiles reaches a correct match between the tiles when the initial relative rotational orientation of the two tiles is in $(-\frac{\pi}{2}, \frac{\pi}{2})$, and the initial relative velocity is in $(0, 1.3m/s)$ (based on tile mass and dimensions) and relative distance between $(0, 2.82m)$ (based on the dimensions of the air-table).

Observe that the top red countour lines, indicating probabilities above 0.04, include a range of relative orientations from roughly -0.5 to 1.5 radians and range of relative velocities from roughly 0.4 to 0.8 m/s. This indicates that the tiles correctly assembly with a probability that is moderately large (at least 0.04) when the tiles have these initial favorable relative orientations ($(-0.5, 1.5)$ radians) and relative velocities ($(0.4, 0.8)$ m/s). This provides some indication of the feasibility of our scheme, since that tile attachment events occur with some moderate frequency in the simulation. However, the stochastic model is very simplified, and in the future physical experiments will be needed for validation.

5.3.2 Scaling of the Simulation System

We consider two types of scaling. In the first interpretation, we consider the relationship between the yield of assembly and the number of component tiles in the system. Intuitively, if the system is too crowded, random collisions are not possible. However, if the system is well mixed such that random collisions are possible, then, the yield of an assembly is directly proportional to the number of component magnetic tiles. We discuss more on yield optimization in Section 5.3.3.

Another interpretation of scale is the length scale. A major limitation to down-scaling our system is the rapid increase of the magnitude of the interactions between magnetic dipoles with the decreasing size of the components [**?**]. The dipole dipole forces are attractive and scale as d^{-4} where d is the distance between their centers. Also, in the nanometer scale, there is a critical length beyond which coercivity almost vanishes and the material becomes superparamagnetic [**?**].

5.3.3 Yield Optimization

Since our low-level physical model leads to a model similar to a chemical kinetics model, it is possible to extract the steady state component distribution and hence use this information to design better tiles. In particular, if we interpret the system as a Markov process then we can use Master's Equation [**?**] to obtain the time evolution of the probability of the system to reach one of the exponentially many configurations. For smaller systems, we can analyze the dynamics of the self-assembling system, in particular calculate system yield by modeling the behavior of the system using a set of difference equations with small degrees of freedom as proposed by Hosokawa et al. [**?**]. For larger systems, we can derive the average behavior of the system using Kolmogorov's Forward Equation [**?**] and, thus, compute the expected number of tiles of each type in the steady state. Based on the Markov Chain interpretation it is also possible to construct a linear program in order to obtain the probabilities that would maximize the yield subject to the rate constraints, as was done by Klavins *et al.* [**?**] for active magnetic assembly. However, our system is essentially passive, hence the best we can do is to use these values to make small changes

in the parameter space and alter the effective on and off rates and hence make incremental improvements to our yield.

5.3.4 Errors in Assembly

Similar to molecular assembly [**?** **?**], errors due to pad mismatch is not uncommon in macroscopic magnetic assembly. Fortunately, the redundancy-based error-correction methods [**?** **?** **?** **?** **?**] developed for the abstract tile assembly model can be applied to this system as well. However, these techniques usually increase the number of distinct components in the self-assembling system and, consequently, its assembly complexity.

For a comparison of our macro-scale magnetic tiling assembly with DNA-based self-assembling systems which inspired the magnetic barcode scheme and has proven a very successful avenue for molecular self-assembly, see section B in the appendix.

6 Summary and Future Directions

While self-assembly has been very successful at the molecular scale, resulting in complex patterning at molecular scales not previously achievable via conventional methods, the use of self-assembly techniques at the macro-scale has so far been limited to the formation of patterns of quite limited complexity due to the very limited variety of adhesive pads that were currently used: namely just positive or negative polarity. In this work we discussed a magnetic force driven macro-scale assembly technique with focus on the assembly and alignment process. We presented the challenges involved in the design of such a magnetic force driven macro-scale self-assembling system, the most important contribution being the design of a barcode scheme which would allow us to generate arbitrary complex structures. In other words, this paper addressed the key challenge of increasing the variety of magnetic pads for tiles, which will allow the tiles to self-assemble into patterns of increased complexity governed by the selection of the pads of the tiles. We presented a physical model based on Netwonian mechanics and Maxwellian magnetics that correctly describes self-assembly of meso-scale tiles using magnetic interaction. We also presented a simulation software system that not only verifies our physical model but also provides

us with the data to extract a higher level thermodynamic model of our self-assembly that is useful for analyzing yields in a large self-assembling system.

One of the immediate goals is to extend the simulation model to a multi-tile system with fans. However, the significance of demonstration of an actual magnetic assembly cannot be underestimated. Hence, one possible future direction is the actual demonstration of the assembly and then a comparison of the experimental and simulation results, particularly the yield and the size of assembly. Another possible direction is to study the potential of a magnetic self-assembling system in three dimensions. The situation becomes more complicated in 3D due to the increase in the degrees of freedom. We would also like to study our encoding technique in a more general manner so that it can be applied to any macro-scale and micro-scale self-assembling system. For instance, one possible direction can be the study of complex self-assembly using the capillary interaction of MEMS tiles patterned with *wetting codes*. Nonetheless, as an enabling technique, our hope is that this assembly approach will be applicable to generic tiles for the generation of arbitrarily complex macro-scale systems.

Acknowledgment

This work is supported by NSF EMT Grant CCF-0829797, CCF-0829798 and AFSOR Contract FA9550-08-1-0188.

A Computing with Molecules

Biological matter is an excellent example of the computational power of molecules. In complex organisms, molecules are used to perform intercellular communication; this form of computation is required for the basic functionality of the organism. Unlike silicon transistors, these processes communicate by means of the physical movement of molecules. Living organisms utilize intricate protein enzymes to perform logic and other computational steps. The field of biomimetics studies living organisms with the goal of duplicating these capabilities. One recent example of such a molecular computing system is a RNAi-based logic evaluator that can operate in mammalian cells [**?**]. In fact, inspired by core biological mechanisms, such as genome replication, gene expression and signal transduction, which manipulate sequence and concentration information stored in molecules, several molecular systems that can process information in new and novel ways have been designed and implemented [**? ? ? ? ?**].

Molecular computing devices have also been built from non-biological matter [**? ?**] such as the electronic switch consisting of a layer of several million molecules of an organic substance called rotaxane. By linking a number of switches developed by Hewlett-Packard Laboratories, the researchers at HP labs produced a rudimentary version of an AND gate. With over a million molecules in a single device, the switches are not technically molecular. Furthermore, they can be switched only one time before becoming inoperable. An improved design corrected this flaw by using a different class of molecules. One related work is the synthesis of a molecule whose electrical conductivity can be altered by storing electrons on demand, thus allowing this molecule to act as a memory device.

A.1 Molecular Self-Assembly

Self-assembly provides one method for fabricating synthetic molecular systems as described in Section A. Molecular self-assembly has a long history of use as a nano-construction process and has recently emerged as a distinct field of academic interest in itself [**?**]. Likely due to an original driving interest in molecular synthesis, macro-scale self-assembly has been studied only recently [**?**]. There have been several demonstrations

of molecular self assembly in the past two decades, including synthesis of self-assembled monolayers [**?**], DNA self-assembled nanostructures [**? ? ? ? ? ?**] and phase separated polymers [**?**].

A.2 Computational Molecular Self-Assemblies

Molecular self-assembly has also been applied to information processing at the nano-scale. Mathematical studies of tiling in fact, date back to 1960s, when Wang introduced his tiling problem which considered whether or not a given set of tiles could tile the plane while following a set of adjacency rules. In 1966 Berger demonstrated that tiling assemblies are capable of universal computation, proving that tiling assemblies are theoretically capable of producing arbitrarily complex structures [**?**]. However, these theoretical ideas were not put to practice until much later.

Seeman [**?**] proposed that DNA nano-structures can be self-assembled by using Watson-Crick complementarity and thus DNA can form the basis of programmable nano-fabrication. A seminal paper by Adleman [**?**] used one-dimensional DNA self-assembly to solve an instance of the Hamiltonian path problem, thus establishing the first experimental connection between DNA self-assembly and computation. This work inspired Winfree [**?**] to apply the theory of Wang tiles to show that two-dimensional DNA self-assembly is capable of performing Turing Universal computation. This proposal was later verified experimentally with the demonstration of a Sierpinski Triangle pattern composed of DNA tiles [**?**].

B DNA-based Molecular Computing vs. Macro-scale Magnetic Assembly

This work on macro-scale magnetic assembly is inspired by our extensive work on DNA self-assembly based molecular computing devices, both theoretical as well as practical. In the context of theoretical results, we have not only proposed methods to improve computation using DNA self-assembly using error-correcting codes [**? ?**] and novel DNA

tile designs [**?**], we have also analyzed extent of damage in fragile DNA nanostructures [**?**] and looked into methods for self-repairing DNA assemblies [**?**]. We have also developed techniques for autonomous molecular computing other than tiling assemblies that allow devices to work isothermally outside controlled laboratory environment [**?**] as well as allow inter-device communication [**?**]. On the experimental front, our group were not only the first to demonstrate DNA self-assembly based computation in one dimension [**?**], but also demonstrated tiling with several novel DNA tiles [**?** **?**] as well as designed and built several DNA based nano-robotic devices [**?** **?**].

Given our extensive experience with molecular assembly, we decided to investigate self-assembly at another scale where all the four cparts of a self-assembling system are different. Typically, a self-assembling system is composed of four key components: *components* that self-assemble, a *binding force* that holds the components together, a *kinetic energy* that drives the assembly process and a *medium* in which the assembly takes place. While our DNA-based self-assembled systems used DNA nanostrctures as components, hybridization as the binding force, temperature change as the kinetic energy and water as the medium for self-assembly, our macroscopic self-assembling system uses very different components: wooden tiles as the components, magnetic force as the binding force, energy from the fans as the source of kinetic energy and air as the medium.

While the barcode scheme and achievable shapes (Section 4.2), combinatorial optimization (Section 4.3.1) and thermodynamic optimization (Section 4.3.2) for tile programming apply to assemblies at all scales, independent of the type of interaction, the physical optimization described in Section 4.3.3 is very specific to our macro-scale magnetic assemblies. Similarly while the techniques of abstracting a kinetic model from the physical model (Section 5.3.1), yield optimization (Section 5.3.3) and error-correction (Section 5.3.4) are applicable to self-assembling systems at a wide variety of scales, the length scale optimization technique (Section 5.3.2) is very much sensitive to the type of interaction used.

In summary, despite all the differences arising from the larger scale, it is still possible to apply many of the self-assembly principles from the molecular scale to our macro-scale assemblies.